Coordination Chemistry Reviews 254 (2010) 2449–2458

Contents lists available at ScienceDirect

Coordination Chemistry Reviews

journal homepage: www.elsevier.com/locate/ccr

Review

Recent advances in instrumentation for absolute emission quantum yield measurements

Hitoshi Ishida[a], Seiji Tobita[b], Yasuchika Hasegawa[c], Ryuzi Katoh[d], Koichi Nozaki[e,*]

[a] Department of Chemistry, School of Science, Kitasato University, Kitasato Sagamihara, Kanagawa 228-8555, Japan
[b] Department of Chemistry and Chemical Biology, Gunma University, Kiryu, Gunma 376-8515, Japan
[c] Graduate School of Materials Science, Nara Institute of Science and Technology, 8916-5, Takayama-cho, Ikoma, Nara 630-0192, Japan
[d] National Institute of Advanced Industrial Science and Technology (AIST), Tsukuba Central 5, 1-1-1 Higashi, Tsukuba, Ibaraki 305-8565, Japan
[e] Department of Chemistry, Graduate School of Science and Engineering, Toyama University, 3190 Gofuku, Toyama 930-8555, Japan

Contents

ARTICLE INFO

Article history:
Received 25 December 2009
Accepted 11 April 2010
Available online 18 April 2010

Keywords:
Emission quantum yield
Fluorescence
Phosphorescence
Ruthenium(II) tris(2,2′-bipyridine) complex
Lanthanide complex
Anthracene
Absolute quantum yield measurement

ABSTRACT

The fluorescence and phosphorescence quantum yields (Φ) of standard solutions have been re-evaluated based on an absolute method using an integrating sphere equipped with a multichannel spectrometer. We have examined in detail the Φ value of ruthenium(II) tris(2,2′-bipyridine) complex which have been often used as the standards in the determination of quantum yields of transition-metal complexes. This revealed that the Φ values for $[Ru(bpy)_3]^{2+}$ were 0.063 in deaerated H_2O, 0.040 in aerated H_2O, 0.095 in deaerated CH_3CN, and 0.018 in aerated CH_3CN, respectively, which are significantly higher than the previously accepted values.

We have also examined the technical aspects in the determination of absolute emission quantum yields for lanthanide complexes and those of organic crystals of anthracene. For the accurate determination for lanthanide complexes, special care must be taken in the spectroscopic measurements because of their narrow absorption and emission bands. For organic crystals, the fluorescence quantum yields are reduced due to reabsorption, chemical impurities and structural defects. Our observations for highly purified anthracene crystals revealed that the lower limit value of Φ was 0.64.

1. Introduction

The recent development of luminescent devices based on organic and inorganic materials, including electro-luminescence devices and lasers, has provided the potential for highly efficient light-emitting system with wide variation of color [1–3]. The emission quantum yield (Φ) is one of the most important parameters to evaluate the potential of novel materials. The Φ value is defined as the ratio of the number of photons of light emitted from a photoluminescent sample to those absorbed by the sample. The most widely used method to determine Φ is by comparing with the standard samples of well examined Φ values. In this method, the emission quantum yield of the sample (Φ_X) is calculated by [4]

$$\Phi_X = \Phi_S \times \left(\frac{I_X}{I_S}\right) \times \left(\frac{F_S}{F_X}\right) \times \left(\frac{n_X}{n_S}\right)^2 \quad (1)$$

* Corresponding author. Tel.: +81 76 445 6606; fax: +81 76 445 6549.
E-mail address: nozaki@sci.u-toyama.ac.jp (K. Nozaki).

0010-8545/$ – see front matter Crown Copyright © 2010 Published by Elsevier B.V. All rights reserved.
doi:10.1016/j.ccr.2010.04.006

where the *I*'s are the integrated emission intensities of the standard and sample solutions under identical conditions. Φ_S is the quantum yield of the standard and *n* denotes refractive index. *F* means fraction of light absorbed. For the determination of accurate quantum yields, however, one must take into account a number of factors, e.g., internal filter effects, self-quenching, reliability of the Φ_S value, and so on. Recording accurate emission spectra is also crucial to the accurate determination. The emission spectra must be corrected for the spectroscopic sensitivity of the spectrophotometer because the sensitivity of the photomultiplier tube (PMT) is not flat with wavelength and steeply decreases outside the 200–800 nm region. The correction can be performed in two ways: use of standard compounds with known corrected emission spectra [5–7] or use of a standard lamp of known color temperature. Even if the spectroscopic sensitivity is corrected, it is hard to avoid the distortion of the spectrum in the near infrared region due to very low sensitivity of PMT and the presence of stray light in spectrometer. Since both the sample and the standard must be recorded under equivalent conditions, it is preferable that the standards have photophysical properties similar to those of samples. When the emission energy or intensity of the standards are so different from those for the samples, further complicated corrections must be required.

In the relative methods, the validity of the Φ values of the standards is important to determine accurate Φ values of samples. The standards must be well characterized and their Φ values should be thoroughly examined [4]. The Φ values of phosphorescent standards are not so reliable compared to the fluorescent ones because phosphorescence intensity is generally air-sensitive and temperature-dependent. Moreover, because phosphorescence generally appears in longer wavelength region than for fluorescence the measurement of accurate spectroscopic profile is more difficult. For the determination of values of Φ in transition metal complexes, phosphorescent complexes of iridium(III) tris(2-phenylpyridine), *fac*-Ir(ppy)$_3$, ($\Phi = 0.40$ in dichloromethane [8]) and ruthenium(II) tris(2,2′-bipyridine), $[Ru(bpy)_3]^{2+}$, ($\Phi = 0.062$ in acetonitrile [9]) have very often been employed as the standard. Adachi and co-workers, however, reported very recently that the Φ value for *fac*-Ir(ppy)$_3$ should be corrected to $\Phi = 0.89 \pm 0.03$ in dichloroethane [10]. Such a large correction of the Φ value has generated considerable confusion in the evaluation of materials for OLEDs. $[Ru(bpy)_3]^{2+}$ ($\Phi = 0.062$) has been used very often as the standard whereas the reported Φ values are somehow scattered in the range from 0.059 to 0.090. The highest value of $\Phi = 0.090$ was determined by Nozaki and co-workers using a CCD based spectrograph and with 9,10-diphenylanthracene ($\Phi = 0.91$) as the standard [11]. Thus, the Φ values of $[Ru(bpy)_3]^{2+}$ should be re-examined thoroughly.

To avoid these errors originating in the Φ values, absolute methods have been developed for the accurate determination of luminescence quantum yield. The first reliable absolute method was developed by Vavilov [12], in which a solid scatterer (magnesium oxide) was used absolutely, to calibrate the detector/excitation system. The Weber and Teale method [13] compares the fluorescent light with light from a scattering solution. This method has the advantage that errors resulting from self-absorption and quenching of fluorescence can be eliminated by extrapolating measurements to zero concentration [14]. Rohwer and Martin developed a diffuse light method which enables accurate measurements with as little as 0.6% of the incident absorbed [15]. As alternatives to optical absolute methods, calorimetric methods [16–19] and photoacoustic (optoacoustic) methods [20,21] have been investigated. These methods detect the fraction of the absorbed energy that is lost by nonradiative processes in a luminescent sample, i.e., the complement of the luminescence energy yield.

Although the absolute methods require performing various complicated corrections, recent advances in instrumentation have enabled the easy and accurate determination of absolute quantum yields. The use of a multi-channel CCD photodetector and holographic gratings allows one to record the precise emission spectrum with minimum distortion even around 1000 nm. The quantum yield measurements using an integrating sphere also enables the evaluation of emission quantum yields for crystals, solids or films.

In this paper, we have re-evaluated the phosphorescence quantum yield of $[Ru(bpy)_3]^{2+}$ using the absolute method. Moreover, we have examined the methodological aspects of the absolute method for the determination of emission quantum yields of lanthanide complexes with very narrow emission bands and those of organic crystals of anthracene.

2. Reevaluation of phosphorescence quantum yields of ruthenium(II) tris(bipyridine) complex using a spectrometer with an integrating sphere and a back-thinned CCD detector

Luminescent metal complexes and inorganic materials have recently attracted much attention because of their utilization in electroluminescence and molecular sensors. A representative example is ruthenium(II) tris(bipyridine) complex ($[Ru(bpy)_3]^{2+}$; bpy = 2,2′-bipyridine) which has interesting and useful photophysical/chemical properties and functions [22,23]. $[Ru(bpy)_3]^{2+}$ exhibits phosphorescence at 550–900 nm at room temperature when excited at the MLCT band around 450 nm (Fig. 1). Since the excited state of $[Ru(bpy)_3]^{2+}$ can be quenched by energy or electron transfer, the ruthenium complex has been utilized as a photocatalyst/sensitizer for photochemical hydrogen evolution and carbon dioxide reduction [24,25].

The ruthenium tris(bipyridine) complex has frequently been used as a standard to relatively determine the quantum yields for emissive metal complexes. However, several different values are reported for the phosphorescence quantum yield of $[Ru(bpy)_3]^{2+}$ in the literatures (Table 1) [9,11,26–32]. Until now, the most frequently cited Φ value for $[Ru(bpy)_3]^{2+}$ in H_2O is 0.042, which was reported by Van Houten and Watts [26,27]. They determined the phosphorescence Φ value relative to that (0.90) of a 0.1 M NaOH solution of fluorescein used as the standard. Nakamaru also reported the identical value by using the same standard [29,30]. Harriman reported a slightly higher value of 0.055 without providing a detailed description of the methodology used to obtain

Table 1
Emission spectral maxima (λ_{em}) and quantum yields (Φ) for $[Ru(bpy)_3]X_2$ in water and acetonitrile at 298 K with their literature values.

X	Solvent	λ_{em}/nm	Φ	Ref.
Cl	H_2O	n.d.	0.042 ± 0.002	Watts [26,27]
n.d.		608	0.055[a]	Harriman [28]
Cl		628	0.042 ± 0.002	Nakamaru [29,30]
Cl			0.028 ± 0.002 (air)	Nakamaru [30]
n.d.		n.d.	0.053	Tazuke [31]
Cl		625	0.063 ± 0.002	Suzuki [32]
Cl			0.040 ± 0.002 (air)	Suzuki [32]
PF_6		626	0.063 ± 0.003	Suzuki [32]
Cl	CH_3CN	611	0.059 ± 0.002	Nakamaru [29]
PF_6		620	0.062 ± 0.006	Meyer [9]
n.d.		620	0.086	Tazuke [31]
n.d.		n.d.	0.090	Nozaki [11]
Cl		621	0.094 ± 0.004	Suzuki [32]
PF_6		621	0.095 ± 0.003	Suzuki [32]
PF_6			0.018 ± 0.002 (air)	Suzuki [32]

n.d.: not described.
[a] The measurement temperature is not described.

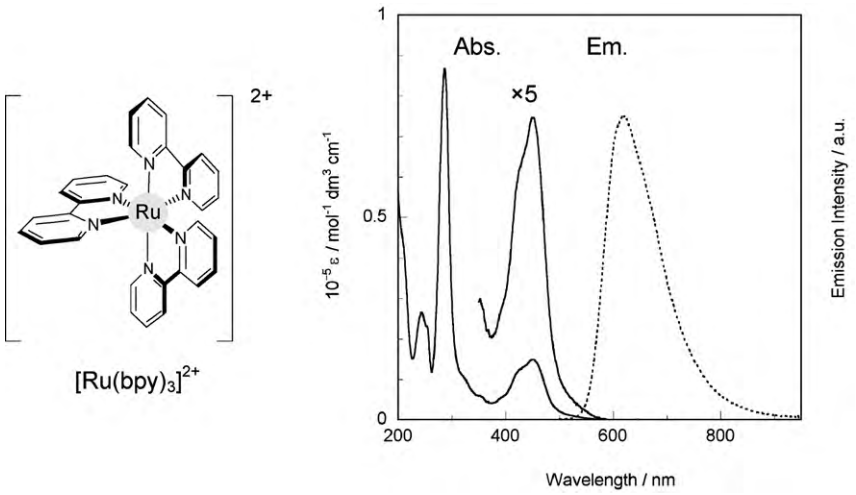

Fig. 1. Absorption and phosphorescence spectra of $[Ru(bpy)_3]^{2+}$ in argon-saturated CH_3CN at room temperature.

this value [28]. Tazuke and co-workers also reported a higher value (0.053) using a spectrometer equipped with a PMT, where the spectroscopic response was calibrated by Lippert's method [31]. Another important value is the phosphorescence quantum yield in air-saturated water, which is frequently utilized by the researchers working in the biological field. Nakamaru reported 0.028, which has often been cited [30].

Various Φ values for $[Ru(bpy)]^{2+}$ measured in CH_3CN have also been reported [9,11,29,31,32]. The representative and the most cited value is 0.062 reported by Caspar and Meyer [9]. This was determined relative to the value (0.042) in H_2O reported by Van Houten and Watts. Nakamaru also reported a similar value (0.059) [29], but Tazuke and co-workers reported a rather higher value (0.086) than those reported so far [31]. These values mentioned above were obtained by using instruments equipped with a PMT. Recently, Nozaki and co-workers reported an even higher value (0.090), which was measured by using a back-thinned charge coupled device (BT-CCD) as the detector and was determined relative to 9,10-diphenylanthracene ($\Phi = 0.91$ in deaerated cyclohexane) as the standard [11].

The methods to determine the luminescence quantum yields can be divided into two approaches: the absolute (or primary) and the relative (or secondary) methods. The relative method is performed by comparing the integrated luminescence intensity of the target molecule with the one of the standard (Eq. (1)). This is usually done without particular corrections. However, if the solvent used for the standard is different from the one for the sample molecule, some corrections in refractive index effects are necessary to determine the quantum yield. Moreover, the emission spectrum of the standard commonly differs from that of the target molecule in the wavelength range used. In this case, careful corrections in the spectroscopic sensitivity of the detection systems are important to determine a reliable quantum yield. On the other hand, the absolute method does not require one to pay attention to the standards. Although the absolute method usually requires complicated corrections, an absolute method that does not need such corrections has recently been developed [15,32,33]. Their systems basically have an integrating sphere to eliminate much of the optical anisotropy by multiple reflections on the inner surface of the integrating sphere.

Fig. 2 shows the schematic drawing of the instrument (Hamamatsu, C9920-02) reported by Suzuki et al. [32]. This system consists of a Xe arc lamp, a monochromator, an integrating sphere, a multichannel detector (the photonic multichannel analyzer, Hamamatsu, C10027-01), and a personal computer. A high reflectance material is mounted on the internal surface of the integrating sphere (99% reflectance for wavelengths from 350 to 1650 nm and over 96% reflectance for wavelengths from 250 to 350 nm). The multichannel detector employs a BT-CCD with 1024×122 pixels and a pixel size of $24\,\mu m \times 24\,\mu m$ providing a wide spectrum range from 200 to 950 nm. The sensitivity of this system was fully calibrated for the region 250–950 nm using deuterium and halogen standard light sources. These standard light sources were calibrated in accordance with measurement standards traceable to primary standards (national standards) located at the National Metrology Institute of Japan.

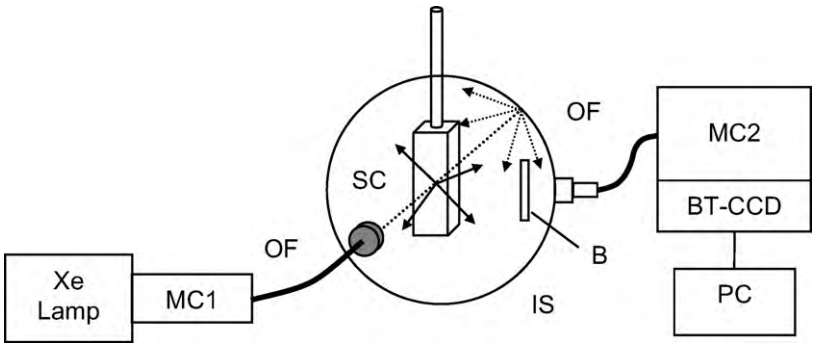

Fig. 2. Schematic diagram of integrating sphere (IS) instrument for measuring absolute fluorescence quantum yields. MC1, MC2: monochromators, OF: optical fiber, SC: sample cell, B: buffle, BT-CCD: back-thinned CCD, PC: personal computer.

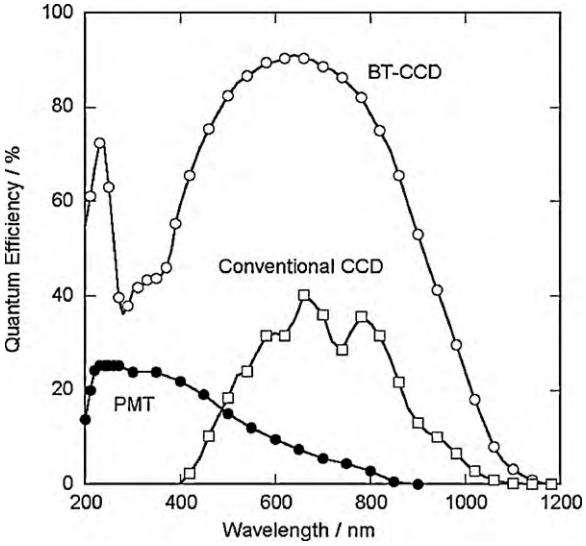

Fig. 3. Spectral response curves for a back-thin CCD (BT-CCD), a conventional CCD and a typical photomultiplier tube (Multialkali).

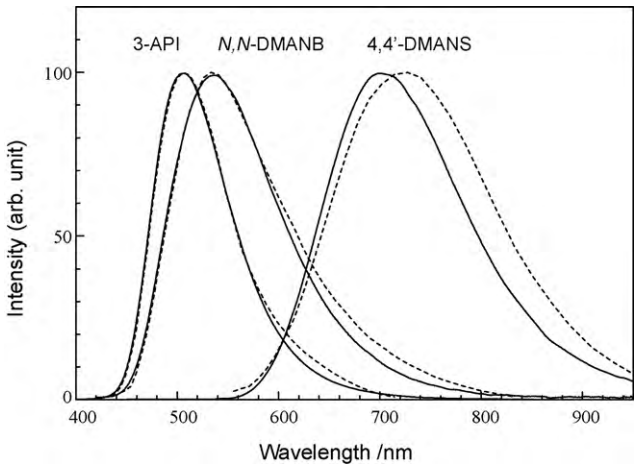

Fig. 4. Fluorescence spectra measured with Hamamatsu C10027-01 [17] (solid lines) in comparison with the reported spectra [22] (broken lines) for 3-aminophthalimide (3-API; 5×10^{-4} M in 0.1N H_2SO_4), *N*,*N*-dimethylaminonitrobenzene (*N*,*N*-DMANB; 10^{-4} M in benzene-hexane (3:7, v/v)), and 4-dimethylamino-4′-nitrostilbene (4,4′-DMANS; 10^{-3} M in *o*-dichlorobenzene).

The quantum yield in the absolute method can be calculated by

$$\Phi = \frac{N_{\text{emission}}}{N_{\text{absorption}}} = \frac{\int \frac{\lambda}{hc}\{I_{em}^{sam}(\lambda) - I_{em}^{ref}(\lambda)\}d\lambda}{\int \frac{\lambda}{hc}\{I_{ex}^{ref}(\lambda) - I_{ex}^{sam}(\lambda)\}d\lambda} \quad (2)$$

where $N_{\text{absorption}}$ is the number of photons absorbed by a sample and N_{emission} is the number of photons emitted from a sample, λ is the wavelength, h is Planck's constant, c is the velocity of light, I_{ex}^{sam} and I_{ex}^{ref} are the integrated intensities of the excitation light with and without a sample, respectively, I_{em}^{sam} and I_{em}^{ref} are the photoluminescence intensities with and without a sample, respectively.

A conventional CCD (i.e., a front-illuminated CCD) generally has low sensitivity in the ultraviolet region, but it has the much better sensitivity at longer wavelengths (the near-infrared region) than that of a typical PMT (Multialkali) as shown in Fig. 3 [34,35]. The BT-CCD used in the instrument reported by Suzuki et al. was improved in the sensitivity at short wavelengths, and it has good sensitivity for luminescence detection in a wide range of wavelengths from the ultraviolet to the near-infrared region. As the higher sensitivity makes the correction factors more reliable, the corrections in the spectroscopic sensitivity of the detection system utilizing the BT-CCD detector are much easier at the long wavelengths than for the PMT detector, which has almost no sensitivity in the near-infrared region.

Inadequate corrections in the spectroscopic sensitivity also cause distortion in band shape of the emission spectra and thus affect the maximum wavelength. Fig. 4 shows the normalized fluorescence spectra of some standards measured with the photonic multichannel detector (solid lines) and the reported spectra (broken lines) [5] for 3-aminophthalimide (3-API in 0.1N H_2SO_4), *N*,*N*-dimethylaminonitrobenzene (*N*,*N*-DMANB in benzene-hexane (3:7, v/v)), and 4-dimethylamino-4′-nitrostilbene (4,4′-DMANS in *o*-dichlorobenzene). The reported spectra were measured by using a detection system equipped with a PMT (RCA, 1P21) (photocathode material (Sb–Cs); the wavelength for maximum sensitivity: 417 nm; 308 and 625 nm for quantum efficiency (QE) 10%; 299 and 667 nm for QE 1%). The spectroscopic sensitivity was corrected with tungsten and mercury standard lamps. Nevertheless, the corrections seem not to be enough particularly in the near-infrared region. For 3-API and *N*,*N*-DMANB which show fluorescence spectra at relatively shorter wavelengths, the reported emission maxima match the spectra measured with the BT-CCD detection system. However, the reported spectra at the longer wavelengths do not match the measured ones. For 4,4′-DMANS showing fluorescence around 700 nm, the measured spectrum differs from the reported one especially at longer wavelengths. In this case, the peak in the measured spectrum is observed at shorter wavelength than the reported one, suggesting that the correction in the spectroscopic sensitivity is difficult in near-infrared region when a PMT is used as a detector due to its low sensitivity in that region. In the reported spectrum for 4,4′-DMANS, the spectroscopic sensitivity could be overestimated at the near-infrared region. However, in general, the emission maximum peak measured by using a BT-CCD detector is observed at a slightly longer wavelength than the PMT, because the PMT does not have enough sensitivity at the near-infrared region.

Suzuki et al. also reevaluated the fluorescence quantum yields of some standard compounds [32]. Although the high sensitivities of the BT-CCD and the corrections in spectroscopic sensitivities at the near infrared region do not always cause the differences between the observed and the reported spectra, there have been differences between the reported quantum yields and those obtained by using Hamamatsu C9920-02. The quantum yields are listed in Table 2 with the values reported so far [4,14,32,36–38]. The reevaluated values for many standards become slightly larger than the reported ones. For example, the quantum yield of 9,10-diphenylanthracene in cyclohexane was reevaluated as 0.97, which is somewhat larger than the reported value (0.9).

Spectroscopic measurements using Hamamatsu C9920-02 were carried out as follows. Fig. 5 shows the excitation light profile and the phosphorescence spectra obtained by setting quartz cells with and without a sample solution, when an argon-saturated acetonitrile solution of $[Ru(bpy)_3]^{2+}$ is set inside the integrating sphere. The irradiation of a quartz cell that does not contain the sample solution gives the excitation light spectrum with a peak wavelength at 450 nm, and the excitation of the sample solution exhibits the phosphorescence spectrum of $[Ru(bpy)_3]^{2+}$ in the wavelength range from 540 to 820 nm, which is accompanied by a reduction in the excitation light intensity. The number of photons absorbed by $[Ru(bpy)_3]^{2+}$ is proportional to the difference of the integrated excitation light profiles, while the number of photons emitted from $[Ru(bpy)_3]^{2+}$ is proportional to the area under its phosphorescence spectrum.

Thus, the quantum yield was estimated to be 0.095 in deaerated CH_3CN [32], which was slightly larger than the value (0.090) reported by Nozaki and co-workers [11]. Similarly, the Φ values for

Table 2
Comparison of Φ values of some fluorescence standard solutions reported by Suzuki et al. [32] with the values in the literatures reported so far [4,14,36–38].

Compound	Solvent	Conc./M	λ_{ex}/nm[a]	Φ_f [17]	Φ_f (reported so far)
Naphthalene	Cyclohexane	7.0×10^{-5}	270	0.23 ± 0.01	0.23 ± 0.02[4]
Anthracene	Ethanol	4.5×10^{-5}	340	0.28 ± 0.02	0.27 ± 0.03[4]
9,10-Diphenyl-anthracene	Cyclohexane	2.4×10^{-5}	355	0.97 ± 0.03	0.9 ± 0.02 [36]
1-Aminonaphthalene	Cyclohexane	5.7×10^{-5}	300	0.48 ± 0.02	0.465 [37]
N,N′-Dimethyl-1-aminonaphthalene	cyclohexane	1.0×10^{-4}	300	0.011 ± 0.002	0.011[37]
Quinine bisulfate	1N H_2SO_4	5.0×10^{-3}	350	0.52 ± 0.02	0.508[38]
	1N H_2SO_4	1.0×10^{-5}	350	0.60 ± 0.02	0.546 [38]
Fluorescein	0.1N NaOH	1.0×10^{-6}	460	0.88 ± 0.03	0.87 [14]
Tryptophan	H_2O (pH 6.0)	1.0×10^{-4}	270	0.15 ± 0.01	0.14 ± 0.02 [4]

[a] Excitation wavelength.

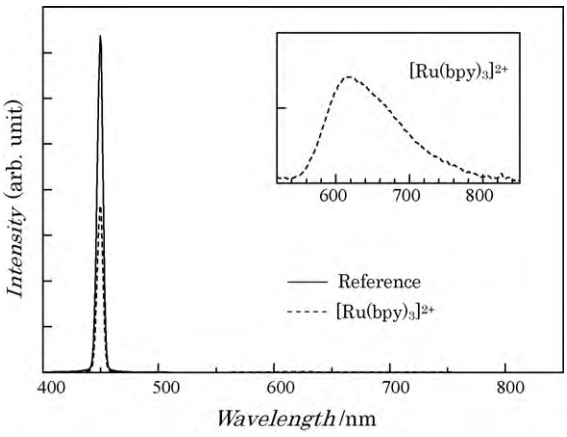

Fig. 5. Excitation light profiles and phosphorescence spectrum obtained by 450 nm excitation of reference (solvent) and $[Ru(bpy)_3](PF_6)_2$ in CH_3CN. The inset is an expanded phosphorescence spectrum of $[Ru(bpy)_3](PF_6)_2$.

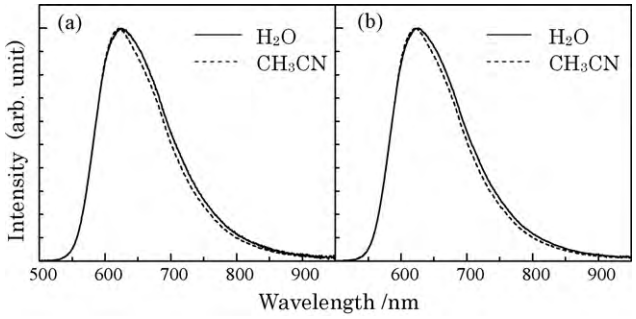

Fig. 6. Emission spectra of (a) $[Ru(bpy)_3](PF_6)_2$ and (b) $[Ru(bpy)_3]Cl_2$ in H_2O and CH_3CN under argon-saturated conditions at 298 K.

$[Ru(bpy)_3]^{2+}$ are reevaluated to be 0.063 in deaerated H_2O, 0.040 in aerated H_2O, and 0.018 in aerated CH_3CN, as listed in Table 1.

From an assumption that differences between the observed and the reported quantum yields may be caused by the difference in the counter anion for $[Ru(bpy)_3]^{2+}$, the phosphorescence spectra of $[Ru(bpy)_3]X_2$ (X = PF_6, Cl) in argon-saturated water and acetonitrile were measured (Fig. 6). Both salts exhibit virtually same phosphorescence spectra with 625 nm in water and 621 nm in acetonitrile, and therefore no effect on the anion counter ions was observed.

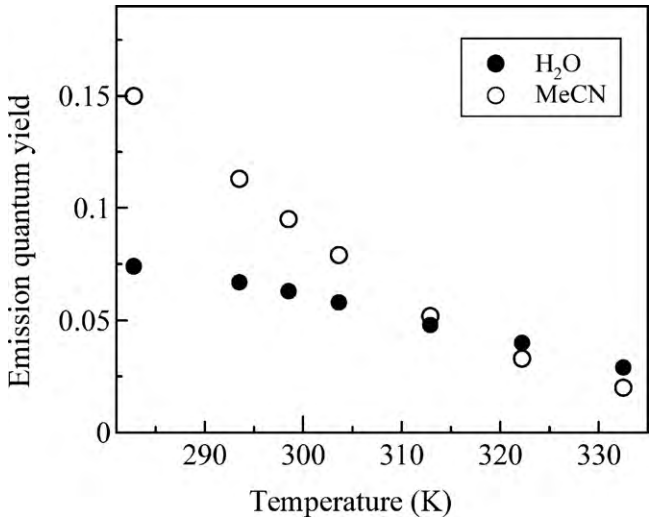

Fig. 7. Temperature dependence of emission quantum yields of $[Ru(bpy)_3](PF_6)_2$ in deaerated H_2O and CH_3CN.

These maximum wavelengths are different from the reported ones: Harriman reported the shorter value (608 nm) [28] and Nakamaru reported the slightly longer one (628 nm) in water [29,30]. In acetonitrile, Caspar and Meyer [9] and Tazuke and co-workers [31] reported similar values (620 nm) but Nakamaru reported a shorter one (611 nm) [29]. The differences in the maximum wavelengths may be attributable to the inadequate corrections in the spectroscopic sensitivity (Table 1).

Differences between the observed and the reported quantum yields may also be caused by the difference in the measurement temperature. From this assumption, the temperature dependence of the quantum yields of $[Ru(bpy)_3]^{2+}$ was examined in acetonitrile and water. As shown in Fig. 7, in which the quantum yields are estimated as the relative to the yields at 298 K, the emission from $[Ru(bpy)_3]^{2+}$ is strongly temperature-dependent around room temperature. It is because of a non-emissive ^{3}d–d excited state lying slightly above the ^{3}MLCT state [39]. With increasing temperature, the non-radiative processes through the ^{3}d–d state become predominant due to thermal population of the ^{3}d–d state. The energy gap between the ^{3}MLCT and ^{3}d–d states for $[Ru(bpy)_3]^{2+}$ depends on the solvent, and is reported to be 37.6–45.7 kJ mol^{-1} (3140–3820 cm^{-1}) [9]. The temperature dependence is larger in

Table 3
Emission quantum yields(Φ), emission lifetimes(τ), radiative rate(k_r) and non-radiative rate(k_{nr}) constants of the Eu(III) complexes.

Complex	Φ	τ/ms	$k_r/10^3$ s^{-1}	$k_{nr}/10^3$ s^{-1}
a: Eu(hfa-D)$_3$(TPPO)$_2$	0.75 ± 0.05	0.71 ± 0.005	1.1	0.31
b: Eu(hfa-D)$_3$(TPPO)$_2$(DMSO-d$_6$)$_n$	0.65 ± 0.11	0.75 ± 0.005	0.86	0.47
c: Eu(hfa-D)$_3$(D$_2$O)$_2$	0.23 ± 0.05	0.41 ± 0.005	0.56	1.9
d: Eu(hfa-D)$_3$(DMSO-d$_6$)$_n$	0.46 ± 0.03	0.86 ± 0.005	0.53	0.63

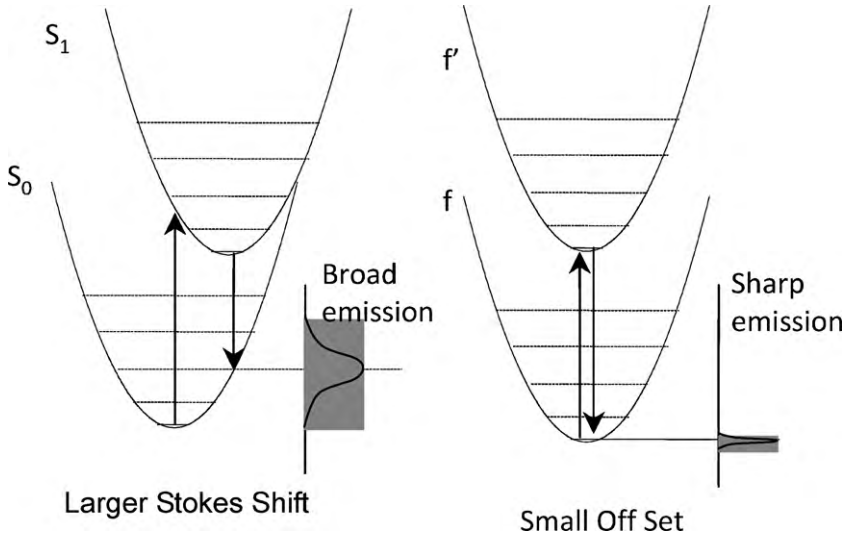

Fig. 8. Comparison of the emission process of lanthanide(III) ions with that of general organic compounds or metal complexes.

acetonitrile than in water, suggesting that careful attention for the temperature is required particularly in acetonitrile in order to obtain reliable quantum yields.

In conclusion, the phosphorescence quantum yields for $[Ru(bpy)_3]^{2+}$ in water and acetonitrile have recently been reevaluated: 0.063 in deaerated H_2O, 0.040 in aerated H_2O, 0.095 in deaerated CH_3CN, and 0.018 in aerated CH_3CN [32]. In the case of $[Ru(bpy)_3]^{2+}$, the BT-CCD, which has much better sensitivity at the near-infrared region than for the conventional PMT, is effective in obtaining the reliable values. Nozaki and co-workers also obtained the quantum yield as 0.090 in deaerated CH_3CN by using another detection system equipped with a BT-CCD and calculating it as the relative value to the fluorescence quantum yield of 9,10-diphenylanthracene in cyclohexane (0.91) [11,40]. However, since Suzuki et al. also reevaluated the fluorescence quantum yield of 9,10-diphenylanthracene to 0.97, the Nozaki's value (0.090) was recalculated to 0.096, which satisfactorily matches with the value (0.095) within experimental error. It is noteworthy that these two separate research groups reached almost the same value using different detection systems. Even after the improved values of the phosphorescence quantum yields for $[Ru(bpy)_3]^{2+}$ were obtained, the current situation, where many researchers were using this complex as a standard to estimate the emission quantum yields, should be improved. All the researchers should pay attention that the phosphorescence and quantum yield for $[Ru(bpy)_3]^{2+}$ are strongly air-sensitive and temperature dependent.

3. Emission quantum yield measurements of lanthanide complexes with narrow emission bands

Lanthanide(III) ions are characterized by an incompletely filled 4*f* orbitals [41,42]. The 4*f* orbitals are shielded from the environment by the filled 5*s* and 5*p* orbitals. Therefore, the influence of the host media on the optical transitions within the $4f^n$ configuration is small. In a configurational coordinate diagram, the potential energy curves of electronic states involved in 4*f*–4*f* transitions appear as parallel parabolas with small displacement as shown in Fig. 8, because the 4*f* electrons are well shielded from their environment [43]. The electronic transitions of lanthanide(III) ions show sharp lines in the absorption and the emission spectra.

Metal complexes with luminescent lanthanide(III) ions, lanthanide complexes are the most popular luminescent materials for application in display devices because of their highly monochromatic clear emission with narrow fwhm (full width at half maxim) [44–49]. In order to estimate luminescent efficiencies of 4*f*–4*f* transition in lanthanide complexes, we have carried out the emission quantum yield measurements using a high-resolution monochromator equipped with an integrating sphere and a PMT. The emission quantum yield values, Φ, were estimated using Eq. (2). The corrected profiles of the light absorption, $I_{ex}^{ref}(\lambda)$ and $I_{ex}^{sam}(\lambda)$ were determined by the excitation spectra of a solvent and a sample solution of Eu(III) complexes, respectively, in the 450–480 nm range, whereas the corrected intensity profile of the emission, $I_{em}^{sam}(\lambda)$, was determined using the emission spectrum (550–750 nm) [50]. According to the measurements of 4*f*–4*f* transition spectra in lanthanide complexes, special notice should be taken of scan rates and slit widths in the emission measurements because of their narrow absorption and emission bands. A typical emission spectrum of lanthanide complex is shown in Fig. 9 [51]. The fwhm of the emission spectrum in the lanthanide complex is estimated to be 1.6 nm which is much narrower than those in organic and transition metal complexes. In order to obtain the absorption and emission spectra with narrow fwhm in lanthanide complex, we have carried out precise measurements (scan rate: 18–60 nm/min, measurement step:

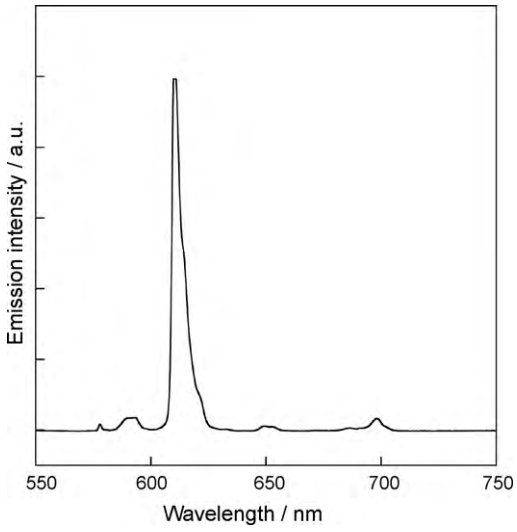

Fig. 9. Emission spectrum of $Eu(hfa)_3(BIPHEPO)$ (hfa: hexafluoroacetylacetone, BIPHEPO: 1,1′-biphenyl-2,2′-diylbis(diphenylphosphine oxide) in acetone-d_6). Excitation at 465 nm.

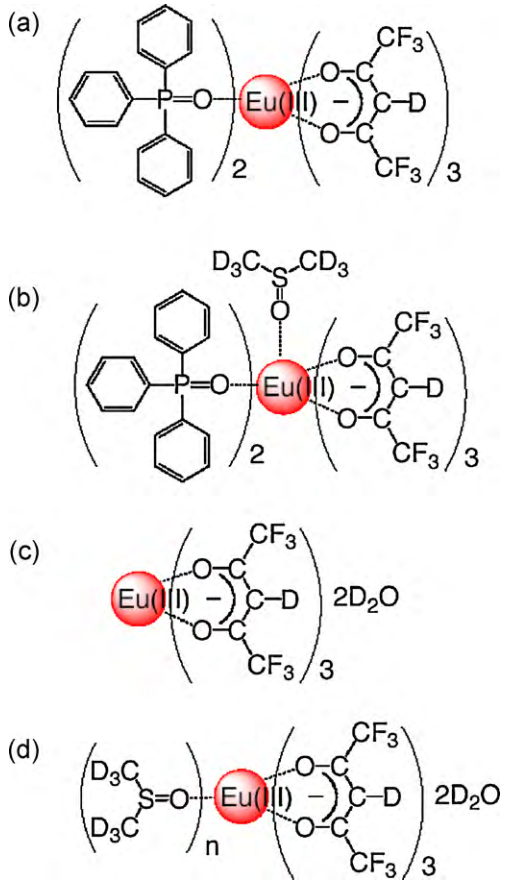

Fig. 10. Chemical structures of Eu(III) complexes. (a) Eu(hfa-D)$_3$(TPPO)$_2$, (b) Eu(hfa-D)$_3$(TPPO)$_2$(DMSO-d$_6$)$_n$, (c) Eu(hfa-D)$_3$(D$_2$O)$_2$, (d) Eu(hfa-D)$_3$ (DMSO-d$_6$)$_n$.

0.1 nm) with the integrating sphere. The emission quantum yields of reference compounds such as Rhodamine 6G determined by the present procedure agreed well with reported values.

We have measured the emission quantum yields of lanthanide(III) complexes for estimation of the luminescent performance. From the emission quantum yields and the lifetimes, the radiative and non-radiative rate constants can be obtained. The radiative and non-radiative rate constants of luminescent Eu(III) complexes in PMMA (polymethylmethacrylate) estimated from the emission quantum yield under excitation at 465 nm (4*f*–4*f* transition) are shown in Table 3 and Fig. 10 [51]. PMMA with high optical transparency is one of the most popular matrices for fabrication of luminescent materials. The non-radiative rate constant of a Eu(III) complex **c**, Eu(hfa-D)$_3$(D$_2$O)$_2$ (hfa-D: deuterated hexafluoroacetylacetonato), is much larger than those of Eu(III) complexes **a**, **b** and **d**. The larger non-radiative rate constant is caused by the higher vibrational frequencies of O-D bonds in coordinated D$_2$O molecules. On the other hand, radiative rate constants of the Eu(III) complex **a**, Eu(hfa-D)$_3$(TPPO)$_2$ (TPPO: triphenylphosphine oxide), is larger than those of Eu(III) complexes **b**, **c** and **d**. Generally, radiative rate constants of the lanthanide complexes depend greatly on the geometrical symmetry of the coordination structure [52,53]. It has been widely accepted that the radiative transition probability between 4*f* electronic configurations is enhanced by reducing the geometrical symmetry of the coordination structure [54–58]. The coordination geometry of Eu(hfa)$_3$(TPPO)$_2$ determined by X-ray single crystal analysis is categorized as a distorted square anti-prism (8-SAP). The characteristic 8-SAP structure is composed of three hfa and two TPPO ligands, which leads to a reduction of the geometrical symmetry of the Eu(III) complex and consequently Eu(hfa-D)$_3$(TPPO)$_2$ shows a relatively large radiative rate constant with highly emission quantum yield.

The radiative rate constants of Eu(III) complexes with DMSO-d$_6$ (Eu(III) complexes **b** and **d**) were smaller than those of complexes without DMSO-d$_6$ (Eu(III) complexes **a** and **c**). Previously, we reported the highest emission quantum yields of lanthanide(III) in DMSO-d$_6$ and polymer matrices by the formation of 12-coordinate lanthanide(III) complex consisting of three hfa ligands and six DMSO-d$_6$ molecules [59]. In the hfa complexes, the coordination of DMSO-d$_6$ molecules with lower-frequency vibrational groups (S=O: 1355 cm^{-1}) prevents the coordination of water molecules having high-frequency vibrational modes which induce radiationless transition. However, the formation of a symmetric 12-coordinate lanthanide(III) complex containing DMSO-d$_6$ molecules leads to reduction of electric dipole moments, so that optical transmissions are dominated by magnetic dipole transitions, which are forbidden by odd parity, resulting in smaller radiative rate constants. Smaller radiative rate constants in the Eu(III) complexes with DMSO-d$_6$ (Eu(III) complexes **b** and **d**) are due to the formation of coordination structure with higher symmetry, such as 12 coordinate.

Emission quantum yields measured under high scan rates (>300 nm/min) and larger slit widths (>5 nm) might be in error by over 50%. The radiative and non-radiative rate constants estimated from the emission quantum yield could be guiding principles for luminescent molecular design.

4. Fluorescence quantum yields of aromatic hydrocarbon crystals

Opt-electronic properties of crystals are different from those of constituent molecules because intermolecular interaction affects such properties. The method to determine fluorescence quantum yields Φ in crystalline phase has been examined using the absolute method with an integrating sphere [60].

For crystalline samples, several factors influence the reliable evaluation of Φ, despite application of the integrating sphere method. Although an apparent quantum yield can be obtained using the integrated sphere method, this value is not necessarily the intrinsic value of the sample material. The following three factors should be taken into account; (1) reabsorption of fluorescence, (2) chemical impurities and (3) structural defects. Reabsorption, which is absorption of fluorescence by the sample, affects the fluorescence properties of crystalline samples. Since absorption spectra at the longer wavelength region overlap with fluorescence spectra at the shorter wavelength region, photons emitted in the bulk of the crystals can be reabsorbed by the crystal. Thus, fluorescence spectra at the shorter wavelength region are suppressed. Since the refractive index of organic materials is sufficiently high, the fluorescence can propagate by a wave-guide effect, leading to efficient fluorescence reabsorption. Reabsorption of fluorescence also occurs during multiple reflections in the integrating sphere [61]. As a result, Φ is reduced because reabsorbed photons are not converted perfectly to fluorescent photons. In the crystalline phase, quenching of fluorescence by impurities and structural defects occurs efficiently because excitons can migrate very efficiently in the crystal. For example, fluorescence of anthracene crystals can be quenched by tetracene doped as impurities at <10^{-6} mol [62]. Here, we show the effect of above-mentioned factors for the apparent Φ of single crystals of highly purified anthracene.

4.1. Effect of reabsorption

For the evaluation of Φ in solution phase, dilute solutions (<10^{-5} mol dm^{-3}) have been used to avoid the effect of reabsorption [32]. Concentration of molecules in anthracene crystal is

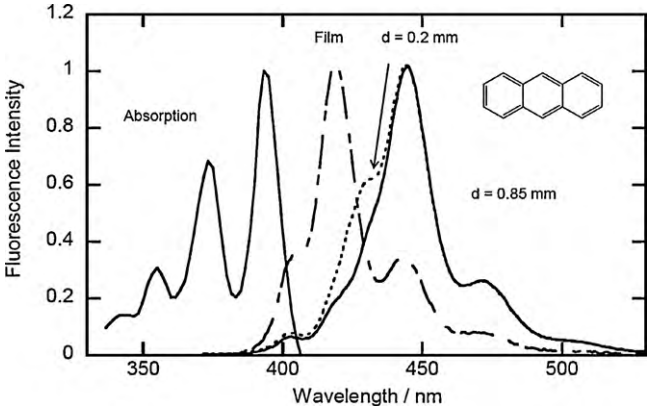

Fig. 11. Fluorescence of thick (solid line), thin crystals (broken line) and spin coated film (dashed line) of anthracene together with absorption spectra.

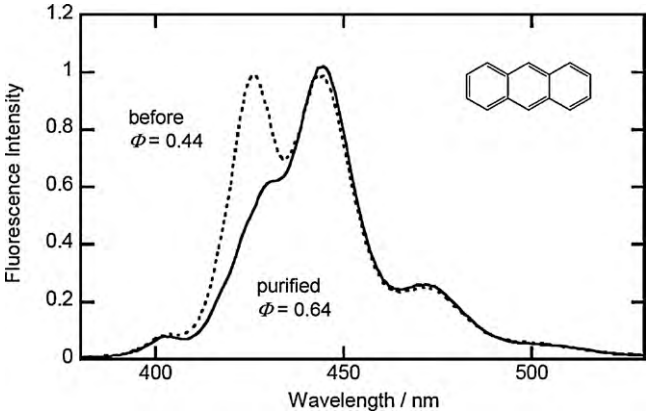

Fig. 12. Fluorescence spectra and apparent Φ for before (broken line) and after purification (solid line).

estimated to be 7 mol dm^{-3} and therefore reabsorption is expected. Reabsorption affects the apparent values of fluorescence properties by suppression of the shorter wavelength region of the fluorescence spectrum, increasing the fluorescence lifetime and decreasing the quantum yield. This is because reabsorbed photons are not converted perfectly to fluorescent photons. The effects of reabsorption have an adverse effect on the reliability of fluorescence spectroscopy for the characterization of organic materials and many studies attempt to minimize these effects [63]. However, no reliable methods have been established.

Fig. 11 shows fluorescence spectra of single crystals of anthracene (thickness d = 0.85 mm (solid line) and 0.2 mm (broken line)) normalized at the peak. Thick samples (d = 0.85 mm) were grown from the melt by the Bridgman method and sample specimens were obtained by cleavage of the crystal ingots. Thin samples (d = 0.2 mm) were grown by a sublimation method. Absorption spectrum of anthracene crystal is also shown. Fluorescence intensity of a thin crystal around 430 nm is slightly stronger than that of thick crystal. This is due to reabsorption effect, namely fluorescence at shorter wavelength range is absorbed by the sample. To discuss this spectroscopic change in detail, fluorescence measurements of spin coated films were examined (dashed line). The thickness of the film was about 100 nm. As shown in Fig. 11, the fluorescence intensity of the film in shorter wavelength range is pronounced. Actually, 0–1 band observed at 420 nm appears clearly, however intensity of 0–0 band is lower than the 0–1 band. This indicates that even for the thinner film (100 nm) the fluorescence spectrum is affected by reabsorption effect, suggesting that Φ is affected by reabsorption.

For single crystals, emitted photons in the bulk of the crystal can propagate in the crystal because of reflection caused by a large difference in the refractive index between crystal and air. As a result, the effects of reabsorption become more pronounced. On this basis, the adverse effects of reabsorption effect are expected to be less pronounced in small crystals. As discuss later, Φ of powder samples prepared by the mechanical milling of the single crystals shows a smaller Φ, indicating that structural defects are introduced by the milling process.

4.2. Effect of impurities

In aromatic hydrocarbon crystals, upon photo-excitation, mobile excitons are generated. There are capture sites, such as impurities and structural defects in the crystals, and therefore quenching of fluorescence by exciton capture occurs efficiently. Exciton capture by impurities have been studied to discuss the diffusion coefficient of exciton. Excitons in anthracene crystals can move rapidly as a result the anthracene fluorescence is quenched by a small amount of tetracene at $<10^{-6}$ mol [62]. It is notable that fluorescence properties are expected to be sensitive to purity of the materials.

Fig. 12 shows fluorescence spectra before and after purification. Purified sample was single crystal and unpurified sample was powder-like sample. Commercially available anthracene (Merck, scintillation grade) was purified by extensive zone refining. Single crystals were grown by a sublimation method. The difference of the spectroscopic shape in the shorter wavelength range is due to differences in reabsorption. As discussed above, reabsorption leads to a decrease of the fluorescence quantum yield. Despite less reabsorption for powder-like samples, Φ of unpurified powder-like sample (0.44) was lower than that of purified single crystal (0.64). This clearly shows that purity of sample is important for the reliable estimation of Φ. As shown in Fig. 12, the spectroscopic shape at longer wavelength range is similar to each other, suggesting that fluorescence quenching occurs by efficient energy transfer of excitons to unemitted impurities. It is notable that Φ can be used as the reference for the purity of organic materials.

4.3. Effect of structural defects

As discussed above, excitons in aromatic hydrocarbon crystals can also be captured by structural defects, which can be introduced by mechanical stress. Thus, we studied the effect of mechanical milling on the fluorescence properties. Mechanically milled samples were prepared by hand using a spatula on the quartz cell.

Fig. 13 shows the fluorescence spectra and Φ together with the fluorescence microscopy images of crystals. The anthracene crystals were prepared by the sublimation method and were 2×5 x 0.2 mm^3 in size. Spectra were normalized at the peak of 445 nm. The fluorescence image of the flake sample before milling revealed fluorescence emitted strongly at the edge of the crystal. This indicates that fluorescence generated in the bulk of the crystal propagates in the specimen and emerges at the edge of the crystal. Fluorescence spectra at the shorter wavelength region became more pronounced by the milling process, suggesting suppression of the reabsorption. However, Φ decreased dramatically from 0.64 to 0.27 by the milling process and the fluorescence spectra at the longer wavelength region became more pronounced. These observations imply that structural defects are formed by the milling process.

There are several candidates for exciton traps induced by the milling process, including surface adsorbed oxygen molecules, surface defects, and defects in the bulk of the crystal. As shown in Fig. 13, the suppression of Φ occurs for millimeter-sized particles. Thus, the formation of surface traps is unlikely, because the exciton diffusion length in anthracene crystals is approximately

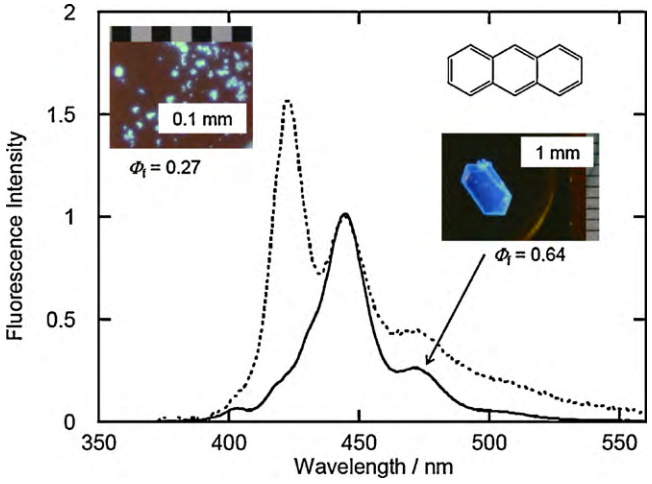

Fig. 13. Fluorescence spectra before (solid line) and after (broken line) mechanical milling process and fluorescence microscopy images for anthracene. These spectra were normalized at the peak of 445 nm.

100 nm [64], which is markedly shorter than the size of the milled crystals (>1 mm). We observed no fluorescence intensity change of powder samples under a nitrogen atmosphere. This observation suggests that structural defects formed in the bulk of the crystals are likely exciton traps. After the milling process, fluorescence at the longer wavelength region becomes more pronounced. This enhanced spectrum is consistent with the spectrum of the anthracene excimer [65]. This observation implies that excitons in the anthracene crystals are trapped by the dimer state of the bulk of the crystals, introduced by the mechanical milling process, and are emitted as excimer fluorescence. The effect of this phenomenon is a reduction in the Φ.

4.4. Comparison with solution value

The Φ obtained for anthracene single crystals (Φ = 0.64) is significantly higher than that in solution (Φ = 0.29 [32]). This observation indicates that a small difference in the molecular properties of solutions and crystals leads to a dramatic difference in the Φ. It should be noted that the values of Φ obtained for solutions cannot used as the Φ value of crystals.

The low Φ of anthracene in solution is based on efficient intersystem crossing (ISC) from the singlet excited state to the second triplet state [66]. Efficient ISC for the anthracene molecule in solution is possible as the energy level of the singlet excited state (E_{S1} = 3.29 eV) is slightly higher than the energy level of the second triplet state (E_{T2} = 3.24 eV). Similarly, some derivatives of anthracene also show a relatively high Φ that is related to the difference between E_{S1} and E_{T2}. A relatively high Φ was observed for crystalline anthracene, suggesting that E_{S1} is higher than E_{T2}. For anthracene crystals, the energy levels of the lowest excited state were reported to be E_{S1} = 3.11 eV and E_{T1} = 1.83 eV [67]. The absorption spectrum due to triplet excitons in single crystals of anthracene has recently been reported, and a broad peak at around 620 nm was observed [68]. By comparing this absorption spectrum with the spectrum of the triplet excited state in solution, the E_{T2} is be estimated to be E_{T2} = 3.51 eV. This energy level is higher than the energy level of the singlet excited state (E_{S1} = 3.11 eV). Thus, the higher Φ of single crystals of anthracene can be explained by inefficient ISC.

5. Summary

The phosphorescence quantum yields for $[Ru(bpy)_3]^{2+}$ in water and acetonitrile were reevaluated using the absolute method. This revealed that the Φ values should be corrected to 0.063 in deaerated H_2O, 0.040 in aerated H_2O, 0.095 in deaerated CH_3CN, and 0.018 in aerated CH_3CN, respectively. When employing these Φ values, however, special care must be taken because the phosphorescence intensity of $[Ru(bpy)_3]^{2+}$ is strongly air-sensitive and temperature-dependent. Furthermore, for the determination of the Φ values using the standard ruthenium complex, we recommend a spectrophotometer with high sensitivity including the near-infrared region and the whole system should be fully calibrated for spectroscopic sensitivity.

For the accurate determination of the Φ values of lanthanide complexes, adequate scan rates and slit widths should be employed in the spectroscopic measurements because of their narrow absorption and emission bands.

The Φ value of highly purified anthracene crystal has been evaluated. The Φ value is reduced by reabsorption, chemical impurities and structural defects. Thus, we measured the quantum yields of single crystals and powder samples prepared by the milling of single crystals. Our observations revealed an estimated lower limit of Φ to be 0.64 for anthracene crystals.

References

[1] W. Brütting, Physics of Organic Semiconductors, Wiley-VCH Verlag GmbH & Co. KGaA, Weinheim, 2005.
[2] L.S. Hung, C.H. Chen, Mater. Sci. Eng. R 39 (2002) 143.
[3] K. Müllen, U. Scherf, Organic Light Emitting Devices, Wiley-VCH Verlag GmbH & Co. KGaA, Weinheim, 2006.
[4] D.F. Eaton, Pure Appl. Chem. 60 (1988) 1107.
[5] E. Lippert, W. Nägele, I. Seibold-Blankenstein, U. Staiger, W. Voss, Z. Anal. Chem. 170 (1959) 1.
[6] R.D. Vocke Jr., Pure Appl. Chem. 71 (1999) 1593.
[7] P.C. DeRose, M.V. Smith, K.D. Mielenz, D.H. Blackburn, G.W. Kramer, J. Lumin. 128 (2008) 257;
P.C. DeRose, M.V. Smith, K.D. Mielenz, D.H. Blackburn, G.W. Kramer, J. Lumin. 129 (2009) 349.
[8] K.A. King, P.J. Spellane, R.J. Watts, J. Am. Chem. Soc. 107 (1985) 1431.
[9] J.V. Caspar, T.J. Meyer, J. Am. Chem. Soc. 105 (1983) 5583.
[10] A. Endo, K. Suzuki, T. Yoshihara, S. Tobita, M. Yahiro, C. Adachi, Chem. Phys. Lett. 460 (2008) 155.
[11] Z. Abedin-Siddique, T. Ohno, K. Nozaki, T. Tsubomura, Inorg. Chem. 43 (2004) 663.
[12] S.I. Vavilov, Z. Phys. 22 (1924) 266.
[13] G. Weber, F.W. Teale, Trans. Faraday Soc. 53 (1957) 646;
D.M. Hercules, H. Frankel, Science 131 (1960) 1611.
[14] W.R. Dawson, M.W. Windsor, J. Phys. Chem. 72 (1968) 3251.
[15] L.S. Rohwer, J.E. Martin, J. Lumin. 115 (2005) 77.
[16] G.A. Crosby, J.N. Demas, J.B. Callis, J. Res. Natl. Bur. Stand., Sect. A 76 (1972) 561.
[17] B. Gelernt, A. Findeisen, A. Stein, J.A. Poole, J. Chem. Soc., Faraday Trans. 2 70 (1974) 939.
[18] M. Mardelli, J. Olmsted III, J. Photochem. 7 (1977) 277.
[19] J. Olmsted III, J. Phys. Chem. 83 (1979) 2581.
[20] S.E. Braslavsky, G.E. Heibel, Chem. Rev. 92 (1992) 1381.
[21] J. Adams, J.G. Highfield, G.F. Kirkbright, Anal. Chem. 49 (1977) 1850.
[22] K. Kalyanasundaram, Coord. Chem. Rev. 46 (1982) 159.
[23] A. Juris, V. Balzani, F. Barigelletti, S. Campagna, P. Belser, A.V. Zewlewsky, Coord. Chem. Rev. 84 (1988) 85.
[24] A.J. Morris, G.J. Gerald, E. Fujita, Acc. Chem. Res. 42 (2009) 1983.
[25] E. Fujita, Coord. Chem. Rev. 185–186 (1999) 373.
[26] J. Van Houten, R.J. Watts, J. Am. Chem. Soc. 97 (1975) 3843.
[27] J. Van Houten, R.J. Watts, J. Am. Chem. Soc. 98 (1976) 4853.
[28] A. Harriman, J. Chem. Soc. Chem. Commun. (1977) 777.
[29] K. Nakamaru, Bull. Chem. Soc. Jpn. 55 (1982) 1639.
[30] K. Nakamaru, Bull. Chem. Soc. Jpn. 55 (1982) 2697.
[31] Y. Kawanishi, N. Kitamura, Y. Kim, S. Tazuke, Riken Q. 78 (1984) 212.
[32] K. Suzuki, A. Kobayashi, S. Kaneko, K. Takehira, T. Yoshihara, H. Ishida, Y. Shiina, S. Oishi, S. Tobita, Phys. Chem. Chem. Phys. 11 (2009) 9850.
[33] L. Porrès, A. Holland, L.-O. Pålsson, A.P. Monkman, C. Kemp, A. Beeby, J. Fluoresc. 16 (2006) 267.
[34] J.R. Lakowicz, Principles of Fluorescence Spectroscopy, 3rd ed., Springer, New York, 2006, p. 45.
[35] From the homepage of Hamamatsu Photonics K.K.: http://jp.hamamatsu.com/en/index.html.
[36] S.R. Meech, D. Phillips, J. Photochem. 23 (1983) 193.
[37] S.R. Meech, D.V. O'Connor, D. Phillips, J. Chem. Soc., Faraday Trans. 2 79 (1983) 1563.
[38] W.H. Melhuish, J. Phys. Chem. 65 (1961) 229.
[39] W.J. Dressik, J. Cline III, J.N. Demas, B.A. Degraff, J. Am. Chem. Soc. 108 (1986) 7567.

[40] S.L. Murov, I. Carmichael, G.L. Hug, Handbook of Photochemistry, 2nd ed., Marcel Dekker, New York, 1993, p. 9.
[41] G. Blasse, B.C. Grabmaier, Luminescent Materials, Review on Luminescence Behaviors, Springer-Verlag, New York, 1994.
[42] F. Gan, Laser Materials, World Scientific, Singapore, 1995, p. 70.
[43] Y. Hasegawa, Y. Wada, S. Yanagida, J. Photochem. Photobiol. C: Photochem. Rev. 5 (2004) 183.
[44] J.-C.G. Bünzli, C. Piguet, Chem. Rev. 102 (2002) 1897.
[45] D. parker, R.S. Dickins, H. Puschmann, C. Crossland, A.K. Howard, Chem. Rev. 102 (2002) 1977.
[46] S.V. Eliseeva, J.-C.G. Bünzli, Chem. Soc. Rev. 38 (2009) 2010.
[47] S. Comby, J.-C.G. Bünzli, Handbook on the Physics and Chemistry of Rare Earths, vol. 37, 2007, p. 217.
[48] R. Reisfeld, C.K. Jorgensen, Lasers and Excited States of Rare Earths, Springer-Verlag, Berlin/Heidelberg/New York, 1977.
[49] M. Gaft, R. Reisfeld, G. Panczer, Modern Luminescence Spectroscopy of Minerals, Springer-Verlag, 2005.
[50] Y. Hasegawa, M. Yamamuro, y. Wada, N. Kanehisa, Y. Kai, S. Yanagida, J. Phys. Chem. A 107 (2003) 1697.
[51] K. Nakamura, Y. Hasegawa, H. Kawai, N. Yasuda, N. Kanehisa, Y. Kai, T. Nagamura, S. Yanagida, Y. Wada, J. Phys. Chem. A 111 (2007) 3029.
[52] M.T. Devlin, E.M. Stephens, M.F. Reid, F.S. Richardson, Inorg. Chem. 26 (1987) 1208.
[53] L. Prodi, N. Zaccheroni, L. Charbonnière, L. Douce, R. Ziessel, J. Am. Chem. Soc. 123 (2001) 12694.
[54] K. Driesen, P. Lenaerts, K. Binnemans, C. Görller-Walrand, Phys. Chem. Chem. Phys. 4 (2002) 552.
[55] W. Liu, T. Jiao, Y. Li, Q. Liu, M. Tan, H. Wang, L. Wang, J. Am. Chem. Soc. 126 (2004) 2280.
[56] J.P. Cross, M. Lauz, P.D. Badger, S. Petoud, J. Am. Chem. Soc. 126 (2004) 16278.
[57] P. Nockemann, B. Thijs, N. Postelmans, K.V. Hecke, L.V. Meervelt, K. Binnemans, J. Am. Chem. Soc. 128 (2006) 13658.
[58] A. Wada, M. Watanabe, Y. Yamanoi, T. Nankawa, K. Namiki, M. Yamasaki, M. Murata, H. Nishihara, Bull. Chem. Soc. Jpn. 80 (2007) 335.
[59] Y. Hasegawa, M. Iwamuro, K. Murakoshi, Y. Wada, R. Arakawa, T. Yamanaka, N. Nakashima, S. Yanagida, Bull. Chem. Soc. Jpn. 71 (1998) 2573.
[60] R. Katoh, K. Suzuki, A. Furube, M. Kotani, K. Tokumaru, J. Phys. Chem. C 113 (2009) 2961.
[61] T.-S. Ahn, R.O. Al-Kaysi, A.M. Müller, K.M. Wentz, C.J. Bardeen, Rev. Sci. Instrum. 78 (2007) 086105.
[62] K. Benz, H.C. Wolf, Z. Naturforsch. 19 (1964) 177.
[63] Y. Nozue, T. Goto, J. Phys. Soc. Jpn. 58 (1989) 1831.
[64] T. Yago, Y. Tamaki, A. Furube, R. Katoh, Phys. Chem. Chem. Phys. 10 (2008) 4435.
[65] W. Rettig, B. Paeplow, P. Herbst, K. Müllen, J.-P. Desvergne, H. Bouas-Laurent, New J. Chem. 23 (1999) 453.
[66] H. Fukumura, K. Kikuchi, K. Koike, H. Kokubun, J. Photochem. Photobiol. A: Chem. 42 (1988) 283.
[67] N. Karl, Landort–Bernstein Numerical Data and Fundamental Relationships in Science and Technology, New Series, vol. 17, Springer, Berlin, 1985.
[68] R. Katoh, Y. Tamaki, A. Furube, J. Photochem. Photobiol. A 183 (2006) 267.